

We are IntechOpen, the world's leading publisher of Open Access books Built by scientists, for scientists

5,500

Open access books available

136,000

International authors and editors

170M

Downloads

Our authors are among the

154

Countries delivered to

TOP 1%

most cited scientists

12.2%

Contributors from top 500 universities



WEB OF SCIENCE™

Selection of our books indexed in the Book Citation Index
in Web of Science™ Core Collection (BKCI)

Interested in publishing with us?
Contact book.department@intechopen.com

Numbers displayed above are based on latest data collected.
For more information visit www.intechopen.com



Aerodynamic Analysis and Design of High-Performance Sails

Sean P. Caraher, Garth V. Hobson and Max F. Platzer

Abstract

High-performance sails, such as the ones used on the America Cup boats, require sails whose aerodynamic characteristics approach those of rigid wings, yet permit a reduction in sail area in high wind and sea conditions. To this end, two-cloth sails are coming into use. These sails are constructed out of an articulated forebody that is a truncated ellipse, the aft of which has sail tracks, or rollers, along the edges to accommodate the twin sails. As the sails on either side need to be of the same length, due to the requirement to sail on different tacks, the two cloth sections need to be of equal length. The requirement then is to have their clews separated and able to slide over each other. More importantly, the transition between the rigid mast section and sails needs to be as aerodynamically smooth as possible in order to reduce drag and hence maximize the lift to drag ratio of the airfoil section that is made up of the mast and twin sails. A computational analysis using ANSYS CFX is presented in this chapter which shows that the aerodynamic characteristics of this type of two-cloth sail are almost as good as those of two-element rigid wing sections. Optimum sail trim configurations are analyzed in order to maximize the thrust production. Applications may soon extend beyond competitive sailing purposes for use on sailing ships equipped with hydrokinetic turbines to produce hydrogen via electrolysis (energy ships). Additionally, high performance sails can be used onboard cargo ships to reduce overall fuel consumption.

Keywords: energy ship, sail aerodynamics, twin-skin sail, computational fluid dynamics, high performance sails

1. Introduction

In his book “The 40-Knot Sailboat” [1] Bernard Smith, the former director of the United States Naval Weapons Laboratory in Dahlgren, Virginia, gives a very illustrative history of the sailing ship development over the past five millennia. It is quite apparent that throughout this long history the cloth sail was considered the obvious best choice because of its ease to adjust to fast changing wind conditions. It is also apparent that the sail aerodynamics remained poorly understood before the pioneering insights of Kutta and Joukowski about the principles of lift generation in the early 1900s. At about this time interest in the sailing ship as a commercially or militarily important technology waned due to the transition to the steamship. Since then, the sailboat is largely regarded as a vehicle of interest only to competitive and recreational sailors. It is therefore not surprising that the cloth sail remained to be regarded as the logical tool to be used for lift, or thrust, generation.

In the early days of aeronautics the very thin foil was also regarded as the most plausible lift generator, inspired by the observation of bird flight. Lilienthal and the Wright brothers pioneered its use and it remained in use until 1917 when the Dutch airplane builder Anthony Fokker showed that relatively thick airfoils provided the German fighter airplanes with better maneuverability in WWI. Since then, their use has become standard practice in aeronautical engineering.

When Bernard Smith began his search for greatly increased sailing speeds in the 1950s he started with the observation: “After centuries of struggle, the fastest sailboats of our time, whether clipper ships, America’s Cup racers, inland lake scows or the amazing double-hulled canoes of the Pacific Islanders, are, after all, only a little faster than the speediest vessels Magellan saw in his day”. He recognized the need for superior aerodynamic sail characteristics offered by modern airfoils and similar characteristics offered by modern hydrofoils. His pioneering developments ultimately led to the “sail rocket” which achieved speeds exceeding 60 knots.

High-performance sails, such as the ones used on the America Cup boats, require sails whose aerodynamic characteristics approach those of rigid wings, yet permit a reduction in sail area in high wind and sea conditions. To this end, two-cloth sails are coming into use. These sails are constructed out of an articulated forebody that is a truncated ellipse, the aft of which has sail tracks, or rollers, along the edges to accommodate the twin sails. As the sails on either side need to be of the same length, due to the requirement to sail on different tacks, the two cloth sections need to be of equal length. The requirement then is to have their clews separated and able to slide over each other. More importantly, the transition between the rigid mast section and sails needs to be as aerodynamically smooth as possible in order to reduce drag and hence maximize the lift to drag ratio of the airfoil section that is made up of the mast and twin sails. Applications may soon extend beyond competitive sailing purposes for use on sailing ships equipped with hydrokinetic turbines to produce hydrogen via electrolysis (energy ships), as proposed in Ref. [2]. In this application it will again be very important to maximize the sail thrust while minimizing the ship drag by means of hydrofoils.

A computational analysis using ANSYS CFX is presented in this chapter which shows that the aerodynamic characteristics of this type of two-skin mainsail are almost as performant as those of two-element rigid wing sections [3]. Optimum sail trim configurations are analyzed in order to maximize the thrust production.

2. Modern sail aerodynamics

The use of sails on large vessels, including cargo ships and tankers, is not a new idea. It has been proposed countless times and many concepts for sail assisted vessels have been proposed [3]. The use of sails may serve to lower carbon emissions from large scale shipping or even be used to harvest energy using hydrokinetic turbines, see References [2, 4]. Generally, the proposed concepts make use of either traditional cloth sails or articulating wing sails. However, the latest edition of the America’s Cup, the most technological advanced sailing competition, may have pioneered another sail configuration that could provide the usability advantages of cloth sails and the performance gains of a rigid wing sail.

The America’s Cup has long been the pinnacle of high-performance sailboat design. Ever since the cup was first competed for in 1851, by the ‘radical’ looking schooner *America*, the race has produced innovations in high performance sailboat design. Rigid wing sails were first introduced to the Cup in 1988 by Dennis Connor’s syndicate. More recently wing sails have been used onboard the AC72 and AC50 catamarans [5]. These rigid wing sails are composed of multiple elements that can

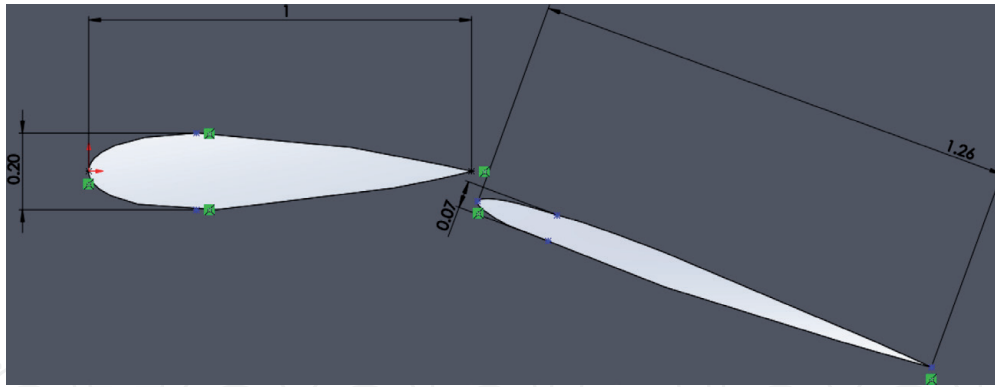


Figure 1.
Possible configuration of a rigid wing sail [6].

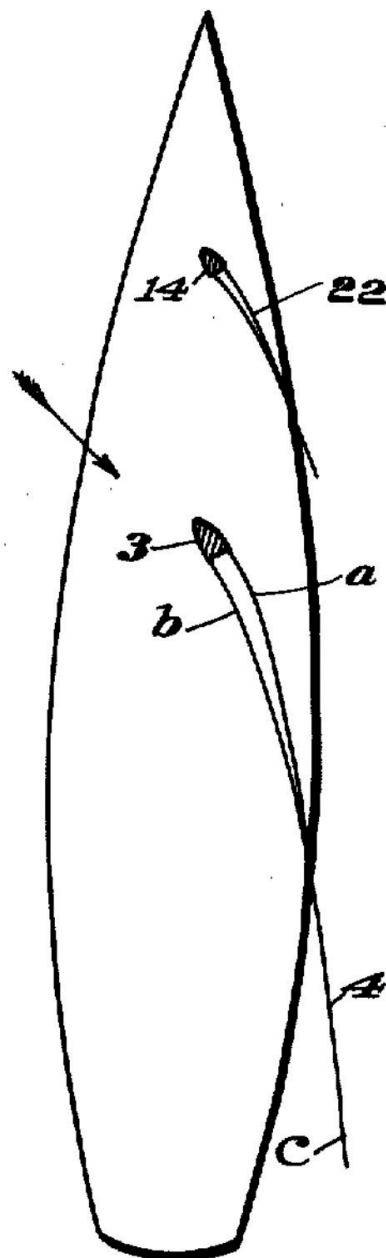


Figure 2.
Drawing from original Herreshoff patent [8].

be articulated to create efficient multi element airfoil sections. **Figure 1** shows the multi-element rigid wing section tested by Johnson. These sails seemed to produce incredible performance for both the AC72 and AC50 classes, however they are held

back by the difficulty of handling a rigid wing. For safe storage these large wings must be taken down in order to prevent them from being damaged by winds while not being used. Their construction generally is very light using an inner carbon structure with a mylar covering. The process of taking one of these sails down took 30 to 40 people approximately one hour with the aid of a large crane in the case of the AC72 wing [7]. In addition, unlike traditional cloth sails, rigid wing sails cannot be reduced or reefed as wind speed increases, which could leave a vessel in a dangerous situation in adverse weather conditions.

These difficulties as well as the increased cost and technical complexity pushed America's Cup organizers to specify the use of a double skin mainsail for the 36th America's Cup. Twin-skin mainsails are not a new concept, however. The idea was first filed for patent by the famous sailboat designer Lewis Herreshoff in 1925, shown in **Figure 2** [8]. This design uses two cloth mainsails that are attached to an elliptic mast section to create an airfoil like shape with finite thickness. The aerodynamic performance of this sail configuration is mostly unknown because most of the development of twin-skin mainsails was done in secrecy by teams competing in the 36th America's Cup. However, these designs seem to promise greater performance than traditional cloth sails without the hassle of a fully rigid wing.

In order to get estimates of the performance that can be expected from these twin skin mainsail sections, a CFD study was conducted on a representative two-dimensional twin skin mainsail section. The analysis was conducted two dimensionally using ANSYS CFX software. The section selected was designed to represent what a twin skin mainsail may look like when hoisted. This chapter will present the results of this modeling and the challenges experienced while attempting to accurately predict the aerodynamic characteristics of the twin-skin mainsail.

3. Discussion of the geometry

The section was designed around the use of a two-to-one elliptic mast section that would serve as the leading edge of the mast. In practice this mast section would be designed to rotate in order to be able to present a smoother airfoil like section for varying angles of incidence. This technique is already used onboard high-performance sailboats and has proven its feasibility in numerous circumnavigations. The sails are then connected to the mast section on either outboard edge. Each sail is of identical chord length so that the configuration can be articulated to accommodate sailing on either tack. In order to induce camber in this section while imposing the condition that each sail is of equal length, the trailing edges are designed to slide over one another. This artificially allows the leeward side of the setup to be moved towards the mast inducing camber into the suction side of the sail. This design is shown



Figure 3.
Twin-skin mainsail geometry.

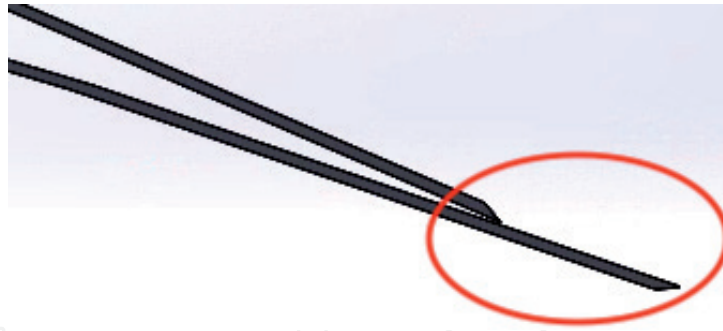


Figure 4.
Trailing edge diagonal cut treatment for simplified meshing.

in **Figure 3**. For ease of meshing in CFD, the trailing edge treatment shown in **Figure 4** was used. This close up also shows in detail how the upper sail is allowed to move forward to induce camber and account for mast rotation.

4. Domain enlargement study

The nature of the boundary conditions in CFD simulations requires the edges of the computational domain to be sufficiently far away from the object being tested. To find a domain size, a simple square domain was created around the proposed geometry. Domain size was slowly increased, and aerodynamic coefficients were monitored. To minimize computational time a small range of angles of attack were chosen for analysis at each domain size. The model was run with inflation layers clustered around the sail providing a non-dimensional distance of the first grid from the sail (Y^+) of approximately one across the entire sail. Y^+ is a non-dimensional distance from wall boundary conditions calculated based on turbulent skin-friction on the wall. For accurate resolution of boundary layer effects, Y^+ should be in the single-digits. For this study the turbulent kinetic energy and dissipation (k- ϵ) turbulence modeling was used to provide a fully turbulent solution.

As domain size was increased (**Figure 5**), measured as the distance to the boundary from the sail, the lift coefficient begins to asymptote as the boundary distance reaches 70 meters, shown in **Figure 6**. In addition, the variation of the vertical velocity along the top of the domain (**Figure 5**) was deemed to be sufficiently small and is shown in **Figure 7**. This leads to a 140 m by 140 m, or

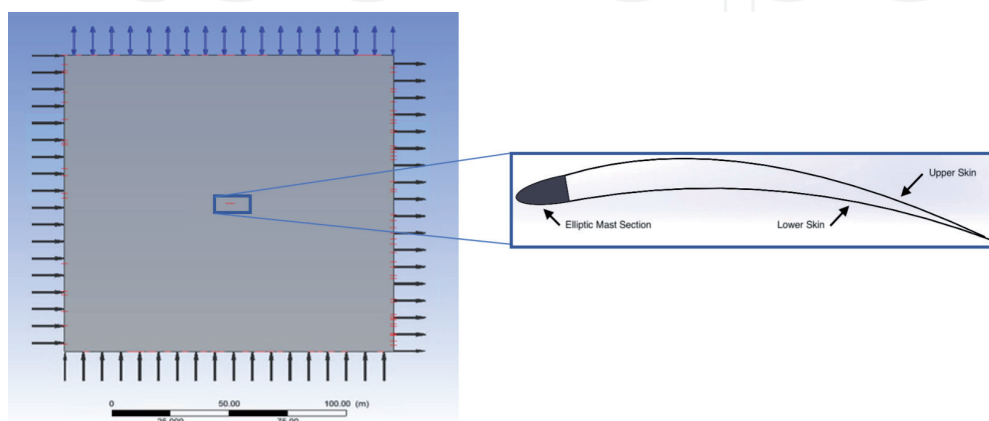


Figure 5.
Configuration of boundary conditions.

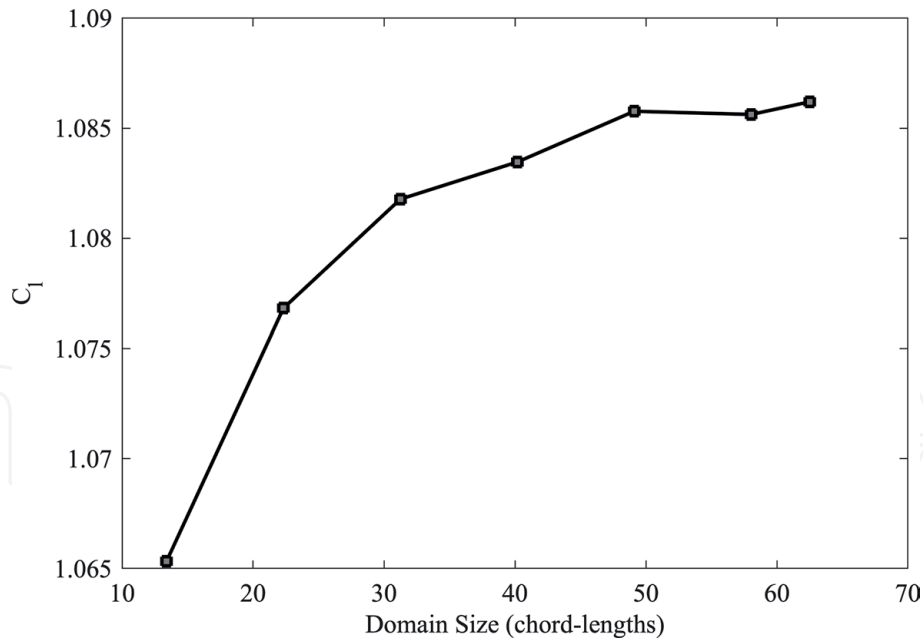


Figure 6. Change in lift coefficient at 2 degree angle-of attack, $Re = 2,000,000$, as domain size is increased.

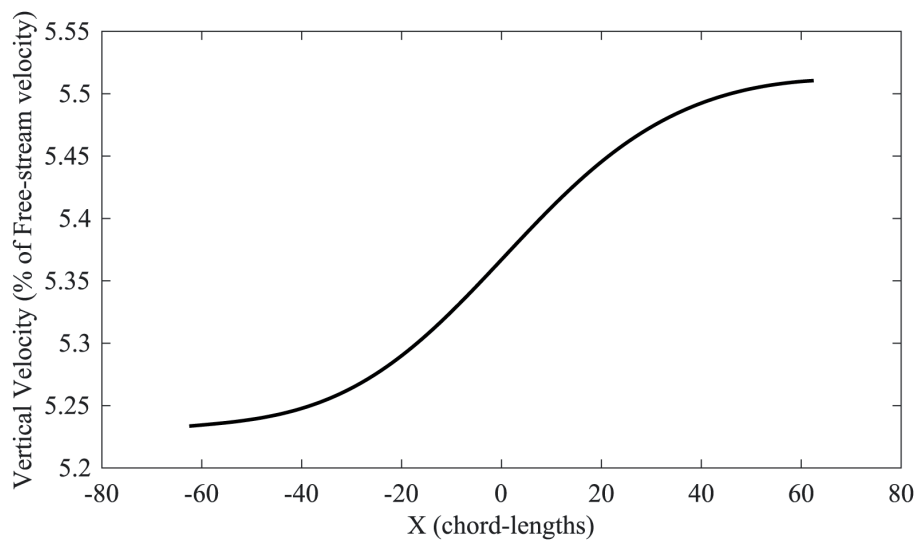


Figure 7. Variation of vertical velocity on the entrainment boundary for 2 degree angle-of-attack.

approximately 60 chord-lengths, domain around the twin-skin sail. From this exploration, it was decided that all future simulations would be conducted with this domain size.

5. CFD setup

From the domain size determined, two different CFX jobs were created. The only difference between them was turbulence modeling. The first job used k-epsilon turbulence with scalable wall functions. The second used Shear Stress Transport model (SST) with Gamma Theta transition. This turbulence model predicts the transition of flow from laminar to turbulent using turbulent kinetic energy and vorticity. The boundary conditions are also shown in **Figure 5** (annotate, Inlet, Bottom, Top, Outlet). The angle of attack was specified by changing the u and v velocity at the inlet boundary condition, which was spread across two faces. An

entrainment boundary condition was located at either the top or the bottom of the domain depending on the angle of attack to allow for circulation affects. Further details regarding this research can be found in Caraher's thesis available through the Naval Postgraduate School, Monterey, California [9].

6. Results

The results from the two different models show stark differences in how aerodynamic coefficients were estimated and how the flow fields behaved. The Shear Stress Transport (SST) turbulence model and Intermittency Momentum Thickness (g - q) transition model struggled to resolve the flow field near stall, shown in **Figure 8** by the inconsistent calculation of lift coefficient above 12 degrees angle of attack. The SST model is a blending of the k - ω (vorticity) and k - ϵ turbulence models, with the k - ω equations being solved near the wall. In comparison the k - ϵ fully-turbulent solution shows a benign stall. This stall begins at the trailing edge as slowly works forward as angle-of-attack is increased, shown in **Figure 9** for the k - ϵ case.

The two models produce different predictions of drag especially at lower angles of attacks, see **Figure 10**. The transition model shows a laminar drag bucket between -5 and 5 degrees angle-of-attack. This drag bucket was unexpected and the sharp increase in drag shown by the transition model occurs over a quarter degree change in angle-of-attack.

This drag bucket is caused by the transition models resolution of laminar flow on the upper surface on the twin-skin mainsail at these angles of attack. This is shown by examining the pressure and skin friction coefficients. Both models predict similar pressure coefficients both in the drag bucket and at higher angles of attack, shown in **Figures 11** and **12**. However, skin-friction coefficients differ within the region of the drag bucket, plotted in **Figure 13**. This plot shows that laminar flow on the lower surface transitions relatively early on the twin-skin mainsail, shown by a sharp increase in skin-friction coefficient as the flow transitions. This area of transition is visible in the flow field as a separation bubble, shown in **Figure 14**. From this point aft, the skin friction coefficients predicted on the lower surface by each model are

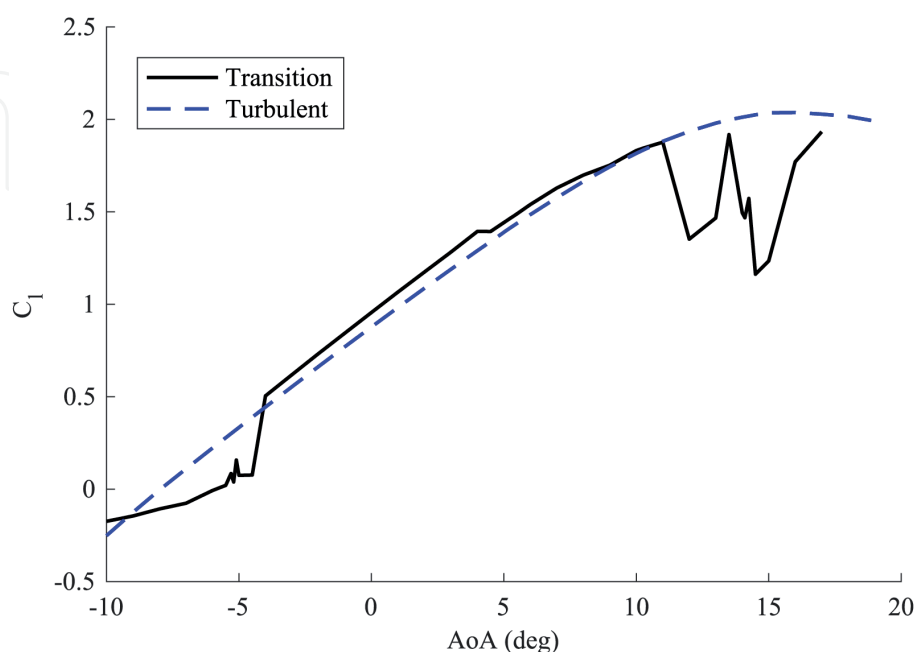


Figure 8.
 C_l comparison between SST and fully turbulent at $Re = 2,000,000$.

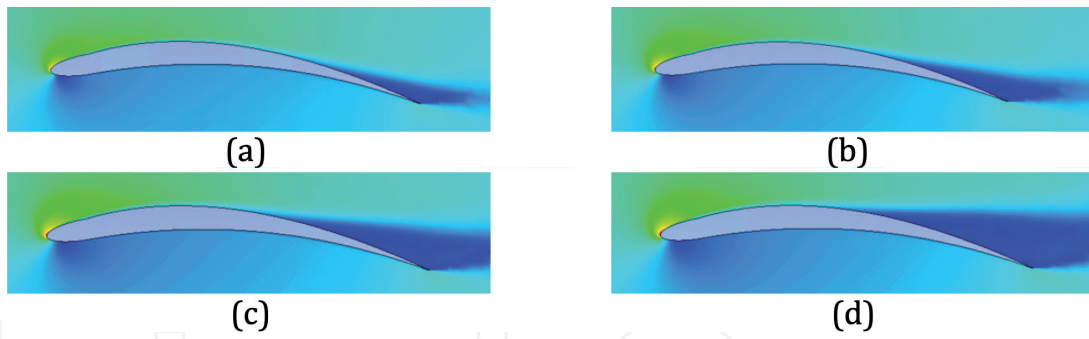


Figure 9. Growth of trailing edge separation in *K-epsilon* model stall. (a) 13 degrees, (b) 15 degrees, (c) 17 degrees, and (d) 19 degrees.

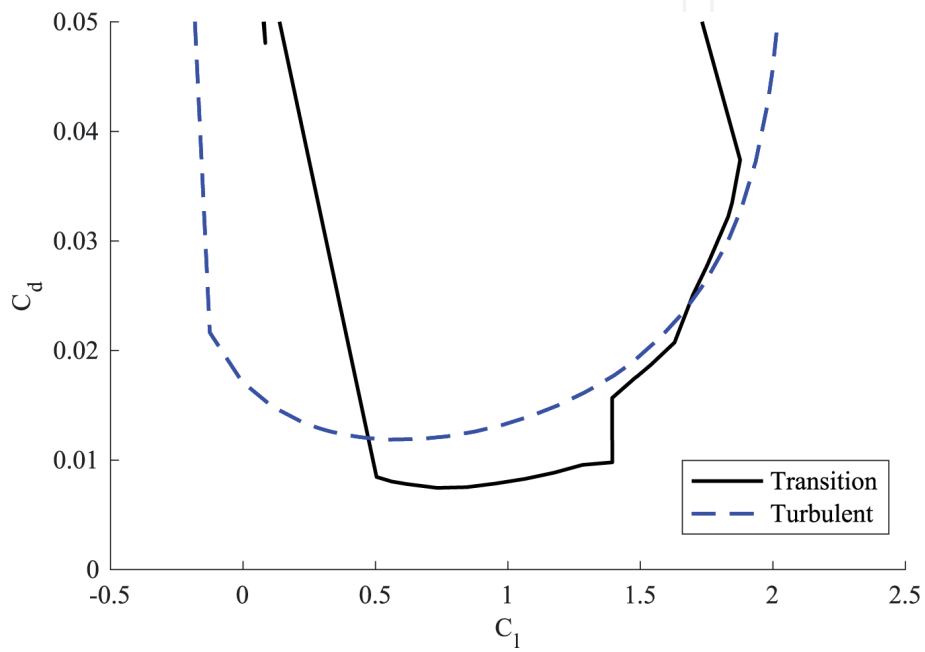


Figure 10. C_d comparison between SST and fully turbulent at $Re = 2,000,000$.

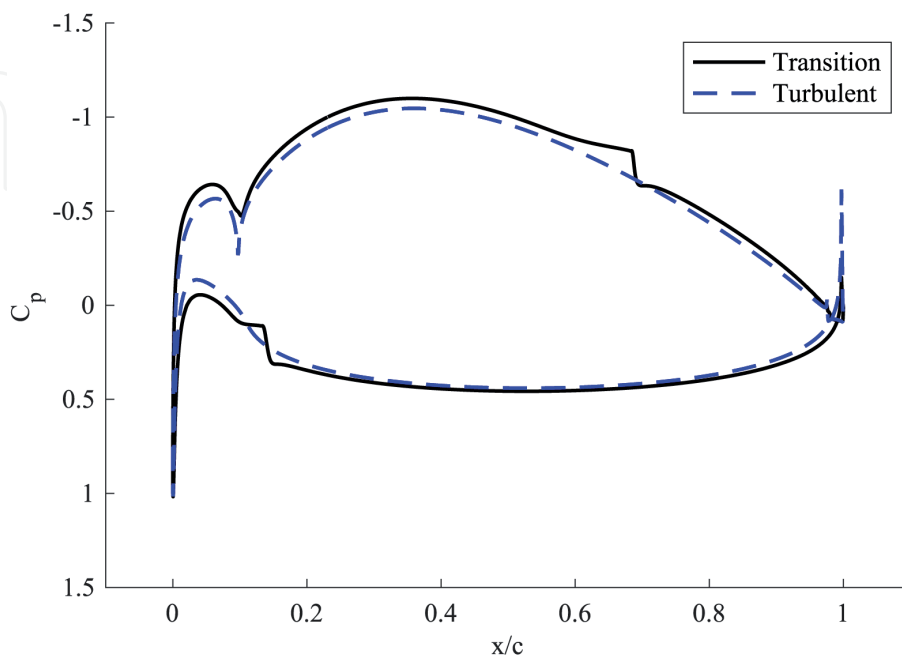


Figure 11. Surface pressure coefficients at $AoA = 1$ degree, $Re = 2,000,000$.

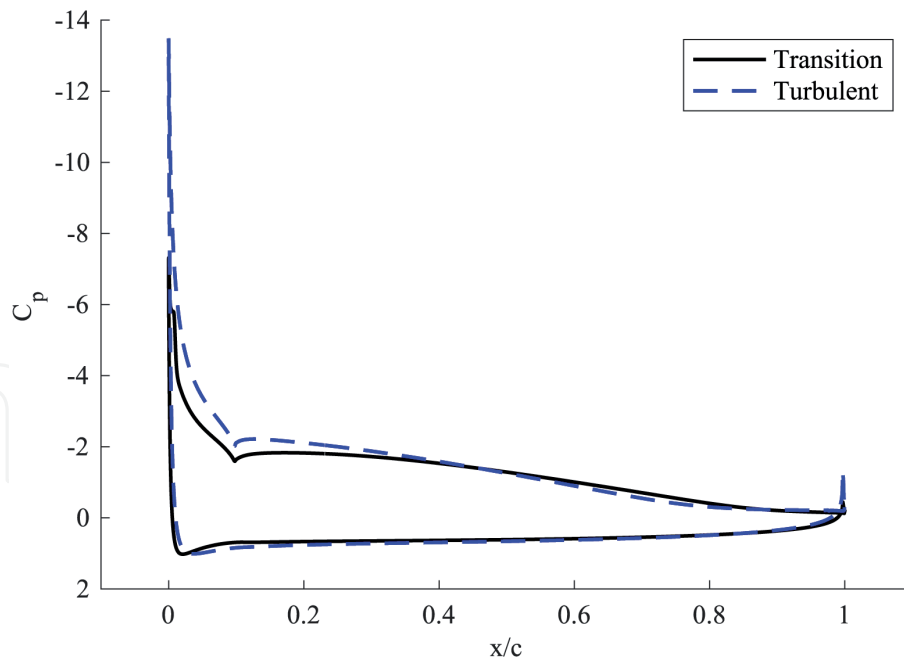


Figure 12.
 Surface pressure coefficients at AoA = 10 degrees, Re = 2,000,000.

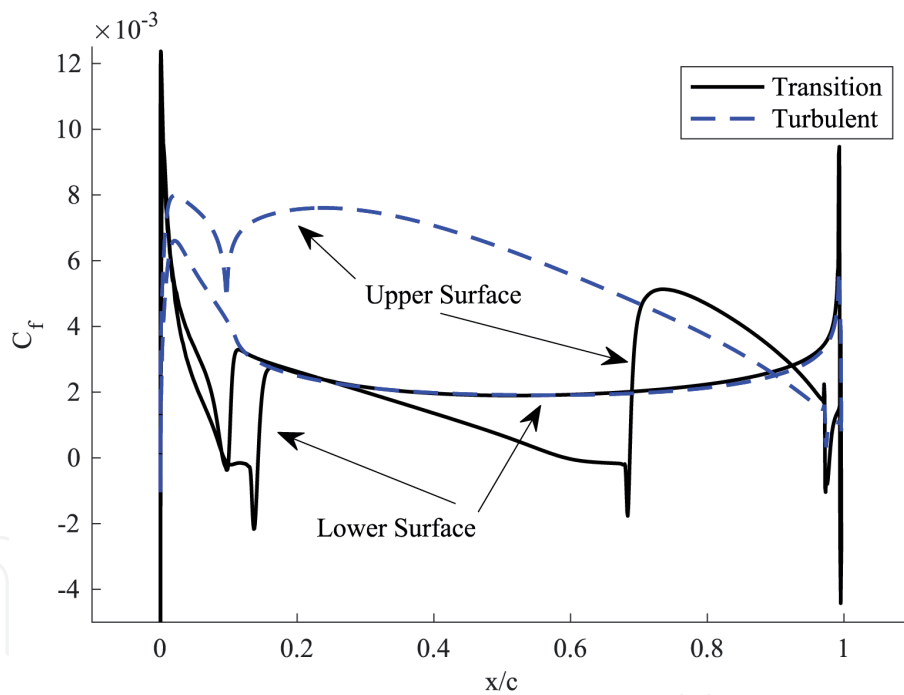


Figure 13.
 Surface friction coefficients at AoA = 1 degree, Re = 2,000,000.

nearly identical. However, the SST model does not predict transition on the upper surface until 70% chord within the region of the drag bucket. This results in much lower skin-friction coefficients on most of the upper surface, shown in **Figure 13**.

At higher angles of attack, laminar flow is no longer predicted along much of the upper surface. In this region, SST predicts transition as the flow accelerates around the leading edge of the mast section, shown as a separation bubble in **Figure 15**. SST's prediction of early transition means that most of the flow around the twin-skin mainsail at higher angles of attack is turbulent, and therefore both models predict similar skin friction coefficients, shown in **Figure 16**. This results in closer prediction of drag coefficients between the two models above 5 degrees angle of attack.

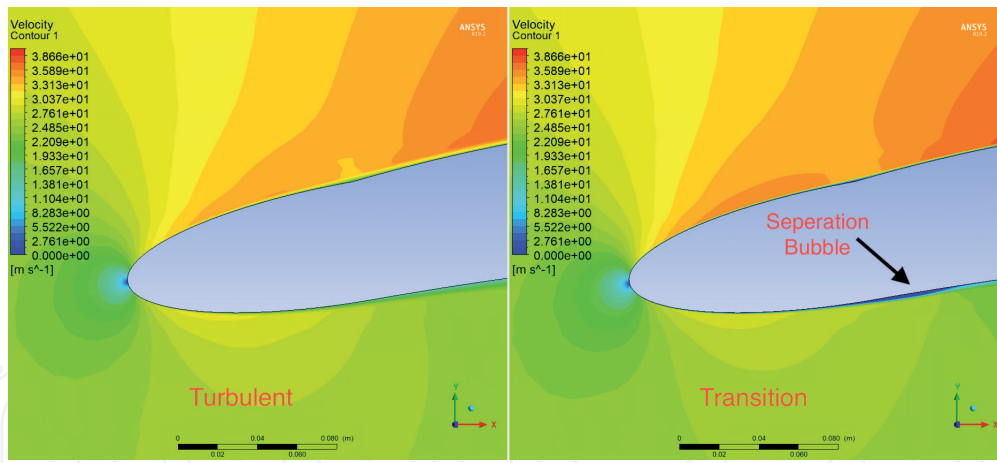


Figure 14.
Leading edge velocity field at 1 degree, $Re = 2,000,000$.

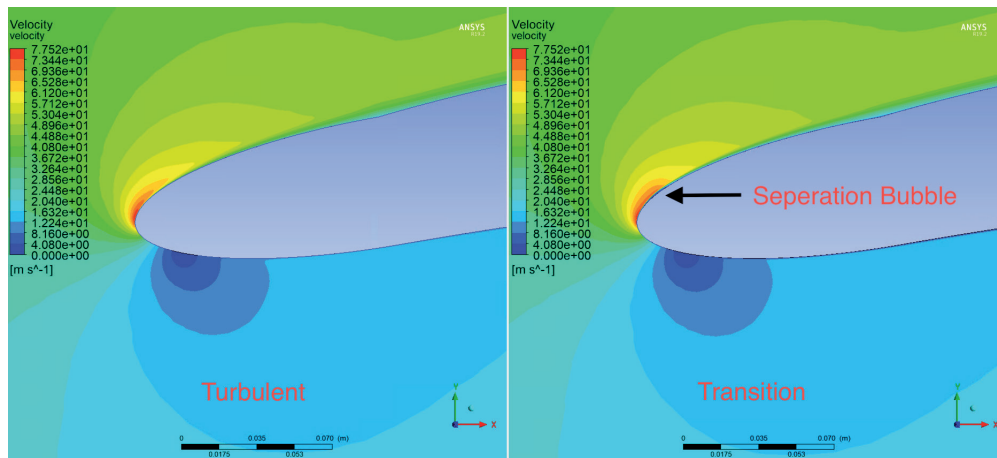


Figure 15.
Leading edge velocity field at 10 degrees, $Re = 2,000,000$.

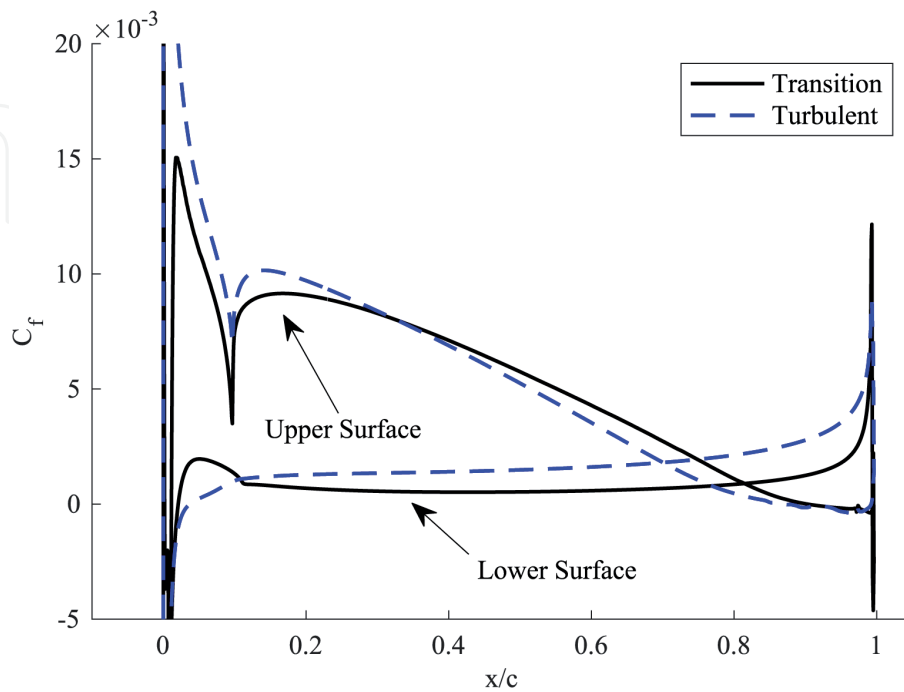


Figure 16.
Surface friction coefficients at $AoA = 10$ degrees, $Re = 2,000,000$.

The environment in which the twin-skin mainsail will be operating dictates that the fully turbulent solution will likely be closer to actual performance. This is due to the constantly changing flow-field that sails experience when deployed. Variations in wind speed and movement of the vessel mean that the velocity and angle of attack that a sail experiences is also constantly varying. This variation will suppress the formation of laminar flow as the chaotic flow-field should favor a turbulent boundary layer. In addition, these models were run without the influence of surface roughness. A real sail will have finite roughness caused by cloth texture as well as imperfections in the surface caused by seams. This should serve as a second factor that should promote turbulent flow around the twin-skin mainsail when deployed.

7. Conclusions

The ANSYS CFX analysis of two-dimensional flow past twin-skin mainsails presented in this paper yielded the following major results:

- a. The sail is able to produce lift coefficients up to a maximum of 2.0
- b. The drag coefficient predictions vary significantly depending on the choice of turbulence and transition modeling. This was to be expected. Nevertheless, a low drag region is predicted in either case between lift coefficients of zero to 1.4.
- c. The twin-skin sail presents the ANSYS CFX analysis with a greater than usual challenge because of the slope discontinuities caused by the transition from the elliptic leading edge to the upper and lower skins and on the upper surface near the trailing edge.
- d. In a previous analysis of the NACA 0012 airfoil [6] the code produced a remarkable agreement with the experiment in the low angle of attack range, thus giving confidence in its ability to predict transitional flows.
- e. The prediction of separation bubbles and the onset of stall requires further detailed study. Fully turbulent calculations predict a rather benign trailing edge stall. If validated in future computational and experimental investigations this feature will be very welcome.

The CFD data that is presented has not been validated by comparison to known data sets. Publicly available data sets concerning the performance of twin-skin mainsails do not exist. These data sets may exist within internal team documentation for the 36th America's Cup, but due to the competitive nature of the event, teams have not published their findings. Despite this there is high confidence that the performance estimations presented in this paper are accurate due to validation of CFX code by Johnson [6].

It appears likely that the twin-skin mainsail will find further application in highly competitive sailing competitions, such as the America's Cup race. In addition, another application may occur in the operation of autonomous sailing ships equipped with hydrokinetic turbines and electrolyzers to produce hydrogen. As explained in Ref. [1], such energy ships require highly efficient sails to produce the propulsive power necessary to overcome the turbine drag and maximize energy production.

When deployed on an ocean-going vessel twin-skin sails should offer an advantage over rigid sails because of ease of stowage and operation. Cloth twin-skin sails can be stowed in either the mast or boom section by rolling the cloth within these sections, unlike rigid sails that cannot easily be stowed. This provides a distinct advantage when operating away from shore in extreme weather and sea-states. By optimizing the sail's performance and aerodynamics, it facilitates the overall system optimization including path planning. In the case of a sail assisted cargo vessel, path planning will consist of optimizing the vessels route to take advantage both weather and sea conditions to minimize fuel consumption.

A detailed investigation into the two-dimensional aerodynamics of a twin skin sail has been completed. The simulations included the effect of computational domain size upon the induced circulation around the airfoil. Additionally, both fully turbulent boundary layer flow as well as transitional flow was investigated. It was hypothesized that sailing ships will likely experience fully turbulent flow over most of the sail due to surface roughness and unsteady flow hence these simulations were most realistic.

Based on the success of the most recent America's Cup competition, twin-skin cloth sails appear to be the most suited to high performance as well as ease of use both in raising and lowering the sails. Hence this concept could be used on large ocean-going ships for either primary propulsion or as auxiliary propulsion to reduce overall fuel burn during transit.

Acknowledgements

The authors gratefully acknowledge helpful comments and advice from Professor Anthony Gannon, Naval Postgraduate School, Monterey.

Conflict of interest

The authors declare no conflict of interest.

IntechOpen

Author details

Sean P. Caraher, Garth V. Hobson* and Max F. Platzer
Naval Postgraduate School, Monterey, USA

*Address all correspondence to: gvhobson@nps.edu

IntechOpen

© 2021 The Author(s). Licensee IntechOpen. This chapter is distributed under the terms of the Creative Commons Attribution License (<http://creativecommons.org/licenses/by/3.0>), which permits unrestricted use, distribution, and reproduction in any medium, provided the original work is properly cited. 

References

[1] B.S. Smith, “The 40-Knot Sailboat”, Echo Point Books and Media, LLC, 1963

[2] M.F. Platzer and N. Sarigul-Klijn “The Green Energy Ship Concept: Renewable Energy from Wind over Water”. Springer Briefs in Applied Sciences and Technology, Springer 2021

[3] C. Delbert, “This Wind-Powered Super Sailboat Will Carry 7,000 Cars Across the Atlantic,” Popular Mechanics, Oct. 07, 2020. <https://www.popularmechanics.com/science/energy/a34272175/wind-powered-sailboat-cargo-shipping-future/> (Accessed May 20, 2021).

[4] N. Gardner, “Brief guide to sail-assisted cargo ships,” Thetius, Sep. 11, 2020. <http://thetius.com/brief-guide-to-sail-assisted-cargo-ships/> (Accessed May 15, 2021).

[5] A. Cup, “History of the AMERICA’S CUP,” 36th America’s Cup presented by PRADA. <https://www.americascup.com/en/history> (Accessed May 06, 2021).

[6] R. Johnson, Susan, Computational aerodynamic analysis of airfoils for energy-producing sailing ships. Calhoun, 2020. [Online]. Available: <https://calhoun.nps.edu/handle/10945/65559>

[7] J. Griffin, “AC75 Double Luff Mainsail,” Sail-World, Aug. 27, 2018. <https://www.sail-world.com/news/209295/AC75-Double-Luff-Mainsail> (Accessed May 06, 2021).

[8] L. F. Herreshoff, “Sailboat,” US1613890A, Jan. 11, 1927.

[9] P. Caraher, Sean, Computational analysis of twin-skin cloth sails for high performance sailing vessels. Calhoun, 2021. [Online].